Publisher: Engineering College, Al Muthanna University
Open Access
DOI:10.52113/3/eng/mjet/2026-14-04-/35-46, Vol. (14), Issue (4), (2026)
Muthanna Journal of Engineering and Technology
MJET
Submitted 28 March 2026, Accepted in revised form 20 July 2026, Published online 23 July 2026

Design and simulation of Multi-Sector Patch Array Antenna For MIMO 5G applications at 3.5 GHz

Shaimaa Kareem Abdallah[a]

[a]*Department of Architecture Engineering, College of Engineering, Al-Muthanna University, Samawah, Iraq, ORCID: https://orcid.org/0009-0004-4747-3814*
**Corresponding author E-mail: shaimaa.kareem@mu.edu.iq*

Abstract

This paper introduces a design of a 5G multi-sector antenna to work at 3.5 GHz, which is the most important band in 5G. The CST studio suite is used to simulate the design and extract the results. The main benefit of using this antenna structure is to get a 360-degree azimuth coverage suitable for macro-cell 5G base station deployment. The antenna operates inside the frequency band (n78 band: 3.3-3.8 GHz), which is used for 5G communications. The design technique involves parametric evaluation of patch dimensions, substrate selection, feed network optimization, and array configuration to reap the highest quality impedance matching and radiation overall performance. Simulation consequences display that the proposed antenna achieves an S11 of better than -18 dB, a gain of 9 dB, and a bandwidth of about 160 MHz, assembling the requirements for 5G base station packages. The multi-quarter configuration permits 360-degree coverage with beam steering abilities, making it a high-quality candidate for macro mobile deployment in 5G networks.

Keywords: *5G Antenna, Patch Array, Multi-Sector, CST Microwave Studio, 3.5 GHz, Sub-6 GHz, Base Station*

1. Introduction

The fifth era of wireless conversation generation (5G) represents a paradigm shift in the telecommunications industry, promising unheard of facts quotes, extremely-low latency, and huge tool connectivity [1]. With top statistics costs concentrated on 20 Gbps for downlink and 10 Gbps for uplink, at the side of latency as little as 1 millisecond, 5G networks are expected to allow a wide range of rising packages consisting of self-reliant automobiles, smart cities, business automation, and immersive digital reality reviews [2].
For providing high speed services, and large data transfer in 5G and 6G, MIMO systems were developed to contain a large number of antenna elements [3].
The successful deployment of 5G networks relies closely at the improvement of superior antenna systems capable of running throughout more than one frequency band. The 3rd era Partnership undertaking (3GPP) has defined primary frequency degrees for 5G New Radio (NR): Frequency range 1 (FR1) covering 450 MHz to 6 GHz (Sub-6 GHz), and Frequency range 2 (FR2) overlaying 24.25 GHz to fifty two.6 GHz (millimeter-wave) [4].
The 3.5 GHz band is the most widely used in 5G network deployments globally, offering a good stability between efficiency and coverage [5].

A microstrip patch arrays antenna, have received a great deal of research due to the great interest in 5G applications, as they have multiple advantages including easy profile, easy of fabrication, light-weight, and compatibility with printed circuit board (PCB) generation [6].
Using an antenna array by combining multiple sectors of the array allows base stations to cover a 360° area and customize the sector to optimize beam radiation patterns, which is essential for 5G base station antennas [7].
The importance of design array antenna for 5G was showed in many article like, design printed array antenna for 5G at band 23-30 GHz by Ahmed and Mahdi [8] and at 60 GHz by Alsawali [9], with a good reflection coefficients less than -10dB over the desired band.

The evolution of antenna era for cell communications has been appreciably documented in the literature. Conventional base station antennas have evolved from easy dipole arrays to state-of-the-art multi-detail phased arrays capable of beamforming and beam steering [10]. Li et al. [11] presented a comprehensive evaluate of mmWave communications for 5G, highlighting the implementation demanding situations and advances in antenna design for excessive-frequency operation.

Many researchers have centered on patch antenna designs for 5G programs. Mounika and Jaya [12] designed a 4x4 microstrip patch array antenna for 5G mmWave programs at 28 GHz, achieving antenna gain of 9.54 dB with high efficiency. Rana and Rahman [13] supplied a micro-strip patch antenna layout for 5G Wi-Fi communique systems at 28 GHz with a go back lack of -38.348 dB and gain of 8.198 dB.
For Sub 6 GHz programs, numerous antenna configurations had been proposed. A compact live-ly planar patch antenna array for sub 6 GHz 5G programs changed into provided with the aid of [14], accomplishing a high advantage of about 17.5 dB at 3.5 GHz. the mixing of energy amplifiers with antenna arrays has proven promising effects for reinforcing transmission electricity and overall machine performance [15].
Multi-sector antenna configurations had been investigated for enhancing base station insurance. A twin band high advantage beam guidance antenna array for 5G sub 6 GHz base station packages was proposed by way of [16], demonstrating the feasibility of attaining dual quarter cover-age from a single panel. Using multi sector antennas reduces the range of required base stations while preserving comprehensive coverage [17].
This paper will present a complete design and simulation study of a multi-sector patch array antenna working at 3.5 GHz for 5G base station programs. The importance of this study is using five sectors microstrip patch arrays to achieve 360-degree multi-sector coverage with high gain per sector (≈ 9 dBi), combined with full MIMO diversity characterization including ECC, diversity gain, TARC, and channel capacity loss. Circular polarization is achieved and verified through axial ratio analysis
This paper simulated the design using CST Microwave Studio , which is used in many articles like[18]. The layout is optimized the usage of CST Microwave Studio, and the overall performance characteristics together with go back loss, benefit, radiation pattern, and bandwidth are very well analyzed. The proposed antenna gives a cost-powerful answer for 5G macro cellular deployment with more advantageous insurance and ability.

2. Antenna structure

The operation of the desired antenna will be explained using patch antenna theory, combined with some general array. Many references define the single patch as a resonant cavity with radiating slots at each line of the patch.
A simple array theory does not take mutual coupling effects into account; it may be used to obtain a first-order approximation of the resulting array pattern of each sector (group of microstrip antennas). The total field of each sector is calculated by the vector addition of the fields radiated by the individual antenna elements. The fields of the different sectors may be combined to form a more omnidirectional radiation pattern.

2.1. Microstrip patch antenna fundamentals

A microstrip patch antenna consists of three layers: ground plane on bottom side, dielectric substrate in the middle, and the radiating patch on top side as shown in Fig. 1 [19].

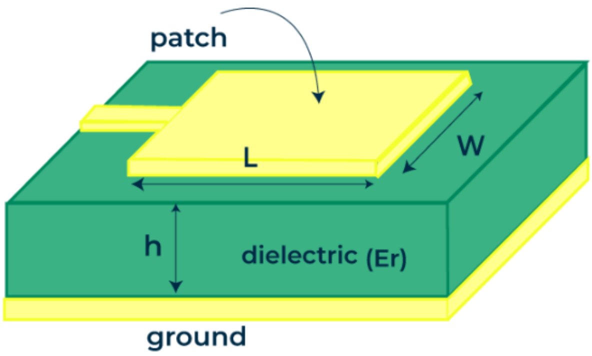

Fig. 1: Microstrip patch antenna structure [19]

The ground plane in microstrip patch antenna is typically made of conducting material such as copper or gold and can take various shapes including rectangular, circular, triangular, or more complex configurations [20]. Using rectangular form in patch is widely used because of its simple design and ease of analysis.
The resonant frequency of a rectangular microstrip patch antenna is determined by the patch dimensions and the substrate properties. The dimensions of patch antenna length (L) and width (W) can be calculated approximated using the following equations [21]:

$$L = \frac{c}{2 f_r \sqrt{\varepsilon_{eff}}} \quad (1)$$

$$W = \frac{c}{2 f_r \sqrt{\frac{2}{\varepsilon_r + 1}}} \quad (2)$$

Where: f_r is the resonant frequency, c is the speed of light, εr is the relative permittivity of the substrate, and εeff is the effective dielectric constant

2.2. Antenna array theory

Antenna arrays merge many radiating elements to generate desired radiation characteristics that cannot be generate from a single element. The total field of an array is the vector sum of fields from all elements, and by controlling the amplitude and phase of excitation to each element, so the radiation pattern can be shaped and steered [22]. The array factor (AF) for an N-element linear array with uniform spacing d is given by:

$$AF = \sin(\frac{N\Psi}{2}) / \sin(\frac{\Psi}{2}) \quad (3)$$

Where: Ψ=k.d.cos(θ)+β , k is the wave number, and β is the progressive phase shift between elements [23].

2.3. Multi-sector patch array antenna structure

The proposed multi-sector patch array antenna is designed to operate at 3.5 GHz, Fig. 2 shows the 3D view of multi-sector patch array antenna. This antenna consists of five array antennas (five sectors) each arranged symmetrically at 72° intervals around the azimuth (0°, 72°, 144°, 216°, 288°), every sector has four microstrip antenna, as shown in Fig. 3.

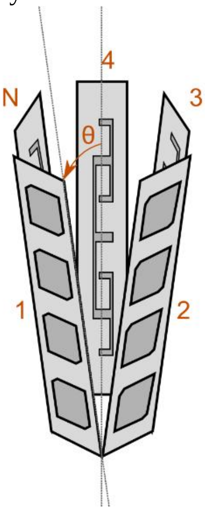

Fig. 2: Multi-sector patch array antenna structure

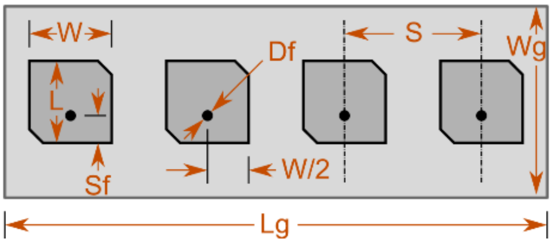

Fig. 3: Antenna sector structure

Single elements of the microstrip pin-fed patch array are fed by vias, connected through holes in the ground plane to a feed network on the underside of the structure, Fig. 4. By varying the pin-inset distance from the edge of the patch along with relevant changes in the corporate feed network, the input impedance can be controlled, without using additional impedance matching circuitry.

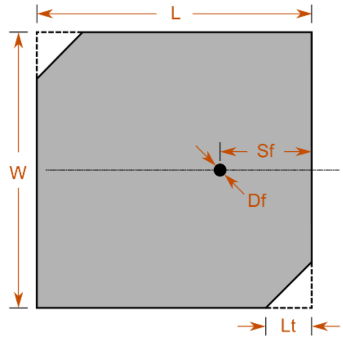

Fig. 4: Microstrip antenna feeding

The four by one microstrip array may be fed using a number of techniques. In this design, the four co-polarized patches of this antenna are fed from a single feed point as shown in Fig. 5.

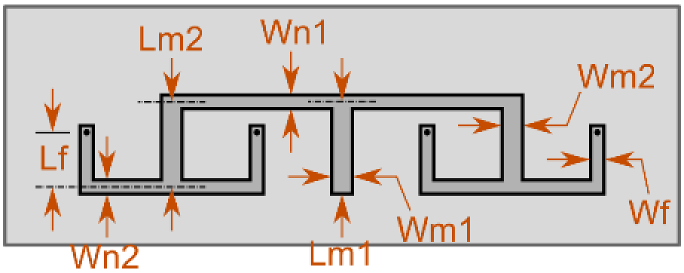

Fig. 5: Antenna array feeding structure

There are many technics to get circular polarization like using various feed arrangements or slight modifications made to the elements, with two orthogonal modes excited with equal amplitudes and 90° time-phase difference.
In this design we use trimming the ends of two opposite corners in a square patch antenna, to get the circular polarization and to achieve quadrature phase coupling between the orthogonal TM01 and TM10 cavity modes.
The patch operates as two half-wave resonators which technicians' position at a 90-degree angle to each other. The process of corner trimming resembles the tuning procedure which changes one resonator to a higher frequency and the other to a lower frequency. At the geometric mean frequency, one is "early" and the other is "late" by a quarter cycle. The combination of these two elements rotates in space because their directional vectors point at 90-degree angles to each other, which produces a movement pattern that resembles two sinusoids separated by a quarter period. The single-feed corner-truncated design achieves circular polarization through its internal design which eliminates the need for external quadrature hybrids and dual feeds, which results in a design that is both compact and easy to manufacture.

3. Antenna design

The choice of substrate material significantly affects the antenna performance. For this design, the substrate with $\varepsilon r = 2$ and thickness 1.74mm is selected. We determine the following specifications: Operating Frequency: 3.5 GHz (n78 band: 3.3-3.8 GHz) with target Gain 9 dB, input impedance 50 Ω, polarization: circular and number of Sectors 5 sectors.

3.1. Single patch design

The initial step involves designing a single rectangular patch element resonating at 3.5 GHz. using the transmission line model equations, the patch dimensions are as follows:
Patch Width (W) = 28.37 mm. Patch Length (L) = 28.37 mm. Feed Point Position = 6.48 mm from edge. We changed the dimension of antenna by using the optimization properties in CST to get best result in reflection loss coefficient S11.

3.2. Array Configuration

The multi-sector configuration consists of five identical 4 patch arrays arranged at 72-degree intervals to provide 360-degree coverage, with θ=0. Each sector array is designed to produce a sectoral radiation pattern with a half-power beam width (HPBW) of approximately 65 degrees in the azimuth plane. The design parameters are as the follows:
Array dimension: Wg=53.3mm, Lg=266.5mm. Other dimensions: S=66.6mm, Sf=6.48mm, Df=0.3mm.

3.3. Feeding design

In this design, the four co-polarized patches of this antenna are fed from a single feed point where the parameters are as the follows:
Wm1=5.78mm, Wm2=3.34mm, Wn1=1.71mm, Wn2=1.71mm. Lm1=15.82mm, Lm2=16.04mm.

4. Results and analysis

This part presents the simulation results calculated by using CST program. The results include return loss (S11), gain, and radiation patterns.

4.1. S-Parameter result

There are five ports for this antenna for five sectors, every sector is similar to other. The reflection coefficient Sii (i is the port number) indicates impedance matching of every sector in the antenna. The Sij (i≠j) indicates the isolation between sectors. Fig. 6 shows the simulated S-Parameters plot for the desired antenna.

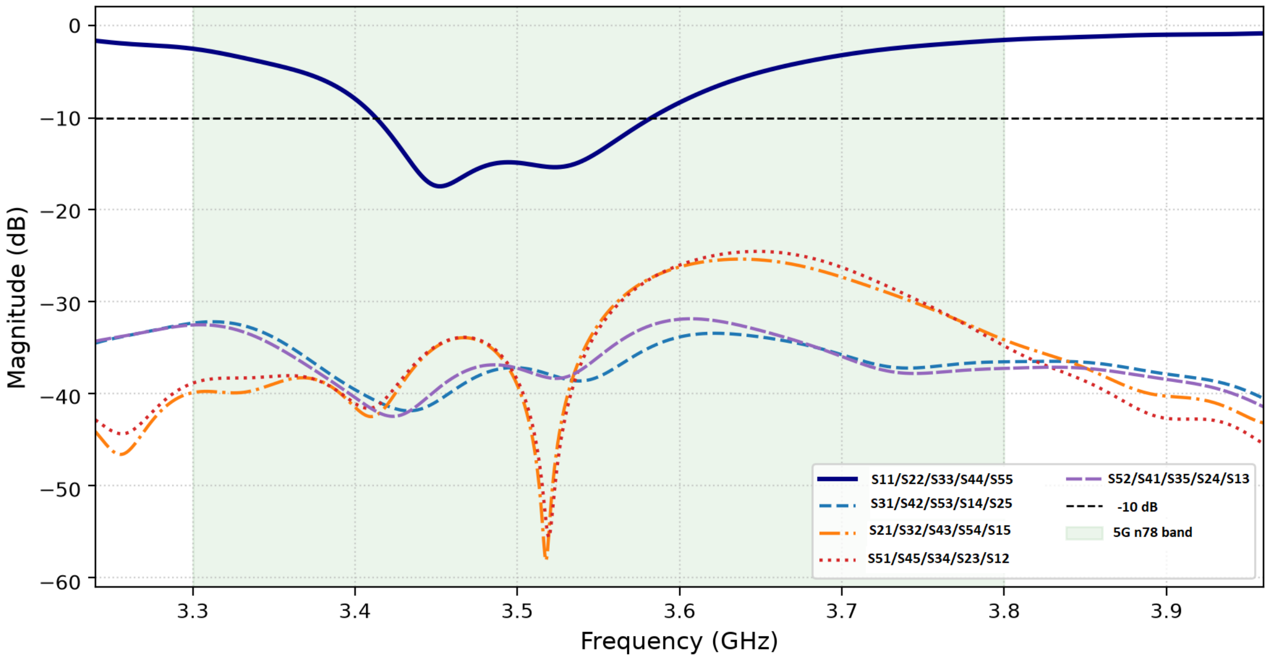

Fig. 6: S-Parameters

The Sii-reflection coefficients are the same for all ports because they have the same design. The bandwidth where Sii less than -10dB is 160Mhz over the band 3.41-3.57 GHz.
The isolation parameters can be divided into two group, one group for two sectors in front of desired sector, and the other group for two sectors near the desired sector. The value depends on the geometry of every sector compared with other sectors. Fig. 7 shows the position of sectors.
The sector 1 has two sectors in front of it (sector 4 and sector 3) so the S31 and S41 almost the same and different from S51 and S21 because the sectors 2 and 5 are near sector1.

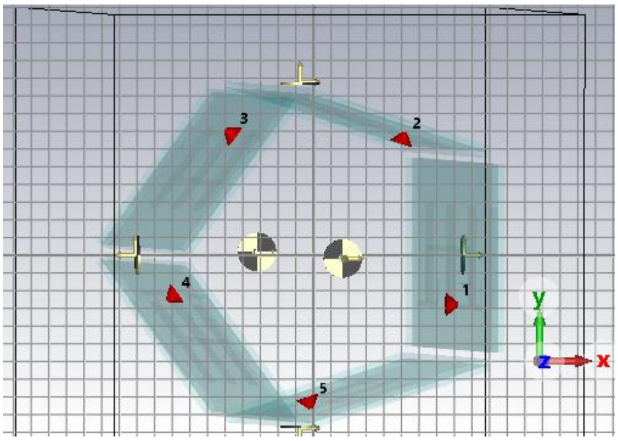

Fig. 7: The position of sectors

4.2. Gain and radiation pattern

The gain and radiation pattern shows the directional characteristics of the antenna. Fig. 8 presents the 2D radiation patterns in the E-plane (elevation) and H-plane (azimuth) at 3.5 GHz. The antenna exhibits a directional pattern with a main lobe directed at theta 90 degrees and reduced side lobes.
Each sector produces a directional radiation pattern with approximately 9 dBi gain and 72° half-power beamwidth (HPBW) in the azimuth plane, which provides a natural 5-sector 360-degree coverage geometry.
The maximum gain is about 9dB which is better than the gain in articles [9], [13], and [18]. When all five sectors are simultaneously active, the combined pattern maintains a gain level exceeding 6 dBi in all azimuth directions (360°).

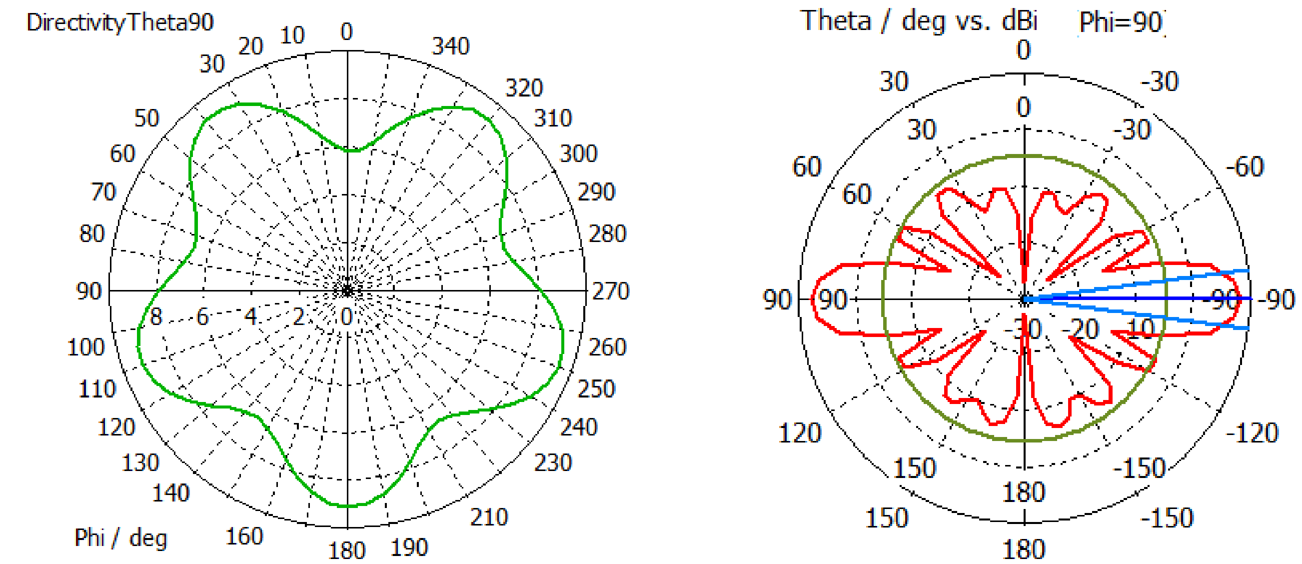

Fig. 8: 2D Radiation Pattern (Polar Plot E-H plane)

The 3D radiation pattern of the desired antenna is showed in Fig. 9. The pattern displays the antenna's ability to focus energy in the 360- direction while suppressing radiation in other directions which is suitable to use in 5G stations.
Fig. 10 shows the total efficiency, which measure of how effectively an antenna converts input power into radiated radio waves, the higher efficiency the less power needed for the same signal strength. This figure shows a good design because the worst case over the desired band is -0.5dB, which mean the efficiency is over 90%.
The maximum gain over the band of frequencies is shown in Fig. 11, where the gain over the desired band is changing from 8.3dBi to 9.3dBi. The change in the gain value is small, which means a good design.

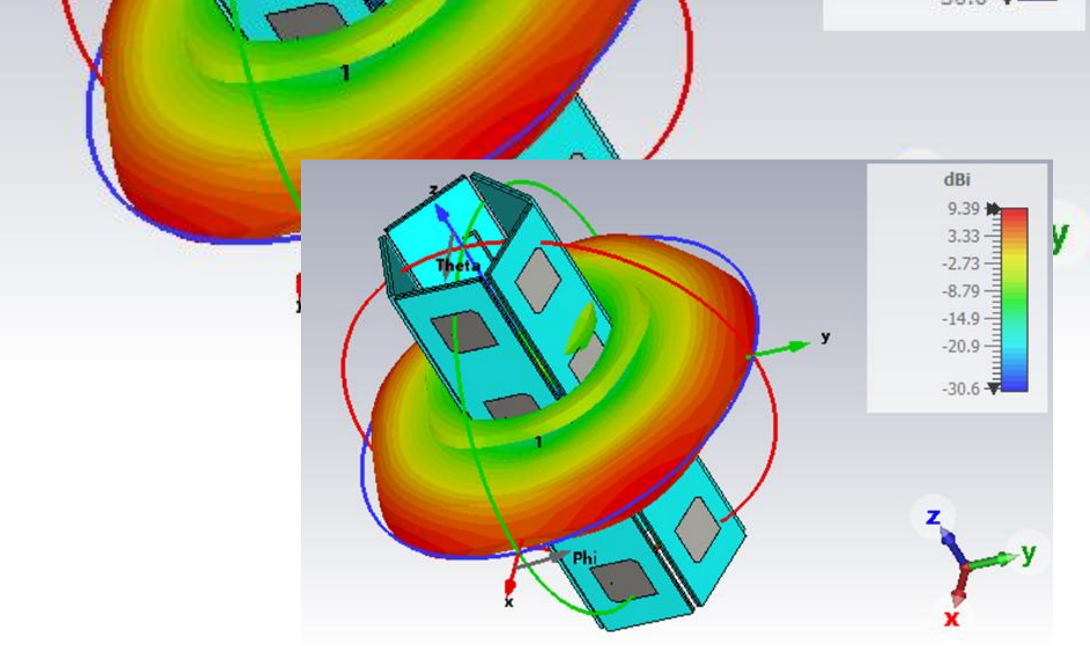

Fig. 9: 3D Radiation Pattern

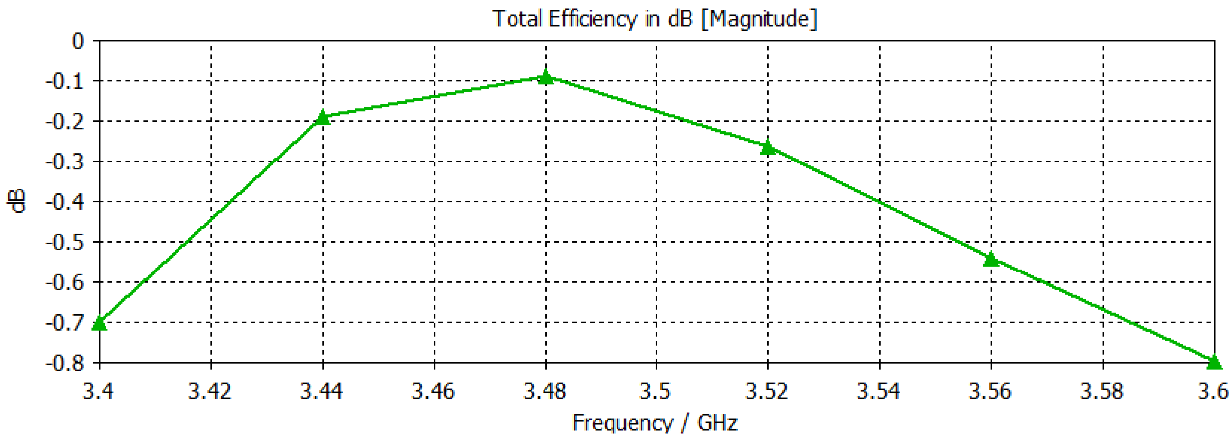

Fig. 10: The total efficiency of the antenna

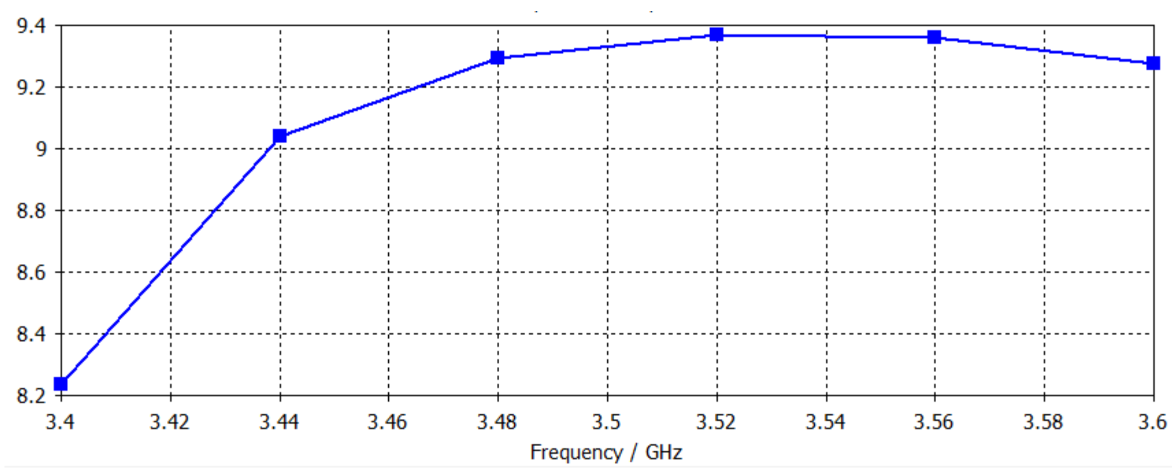

Fig. 11: The maximum gain over the band of frequencies

Through the axial ratio (AR) analysis, the circular polarization can be verified. Fig. 12 shows the simulated AR versus frequency from 3.3 to 3.9 GHz.

the AR radiation pattern at 3.5 GHz is less than 3 dB, confirming circularly polarized radiation in the intended coverage direction.

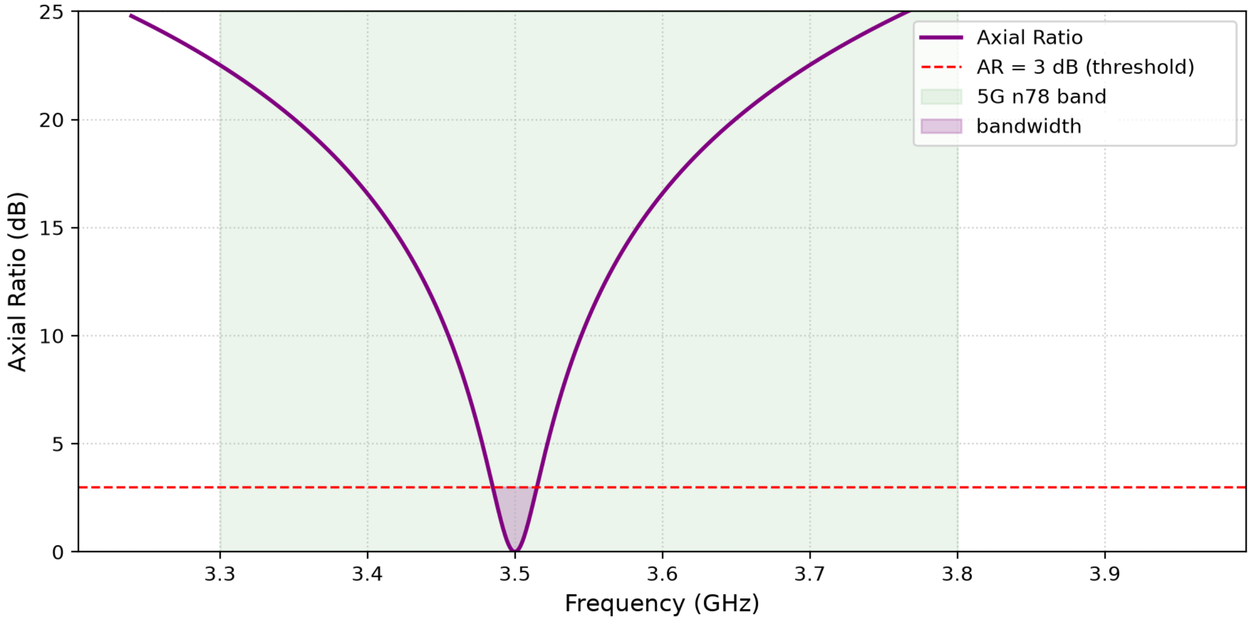

Fig. 12: Axial Ratio vs. Frequency

4.3. The Distribution of Surface Current

The benefit of the surface current distribution is to show the power flowing from antenna and provides insight into the radiation mechanism and helps identify potential areas to improve the design. For the desired antenna the main power flow is from the patch antenna and feeding line as showed in Fig. 13 at frequency 3.5 GHz. Uniform current distribution across all patches indicates phase synchronization and a good feed network design.

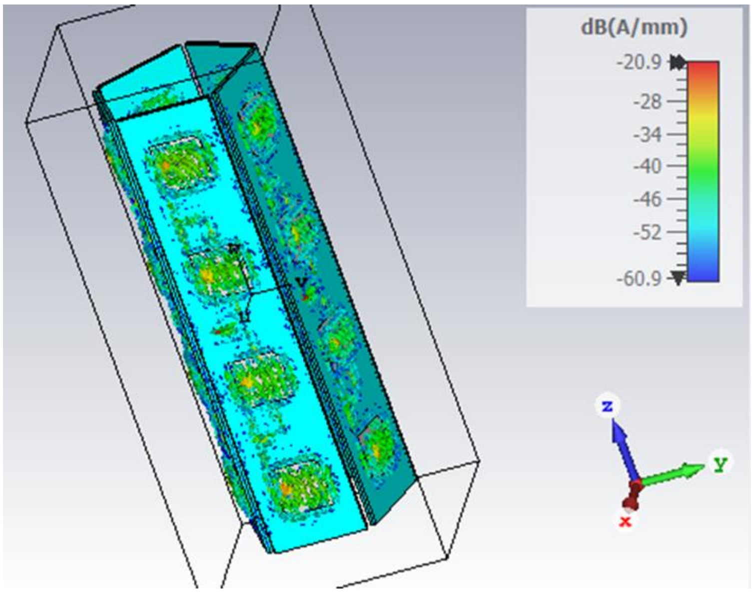

Fig. 13: Surface Current Distribution

4.4. The MIMO Performance Analysis

To fully analysis the multi-port (MIMO) performance of the five-sector antenna, the following key MIMO metrics are computed over the frequency range 3.3–3.9 GHz.

Fig. 14 shows the envelope Correlation Coefficient (ECC), where ECC quantifies the degree of correlation between antenna ports. The ECC remains good below 0.01 for all port pairs across the entire 3.3–3.9 GHz band (limit: ECC < 0.5 for MIMO, ECC < 0.01 for high-performance systems). This confirms excellent port decorrelation enabled by the 72° angular separation between sectors.

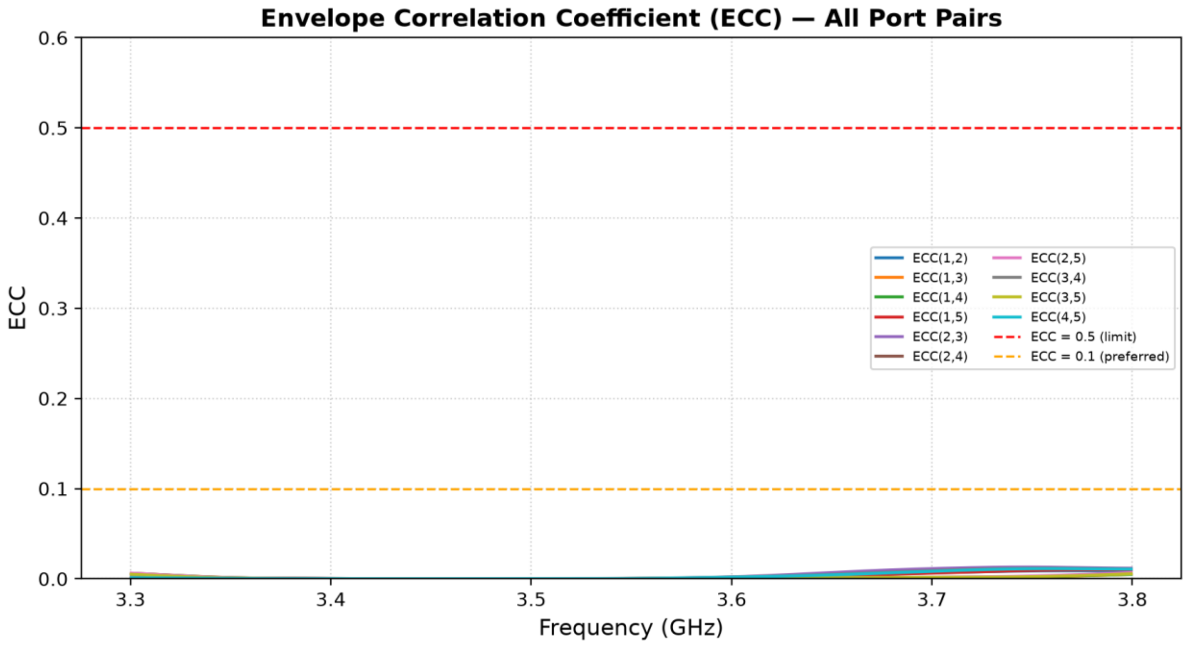

Fig. 14: Envelope Correlation Coefficient (ECC)

The second parameter is Diversity Gain (DG)**,** Fig**.** 15 shows DG exceeds 9.99 dB for all port pairs across the band, confirming that the multi-sector design effectively exploits spatial diversity.

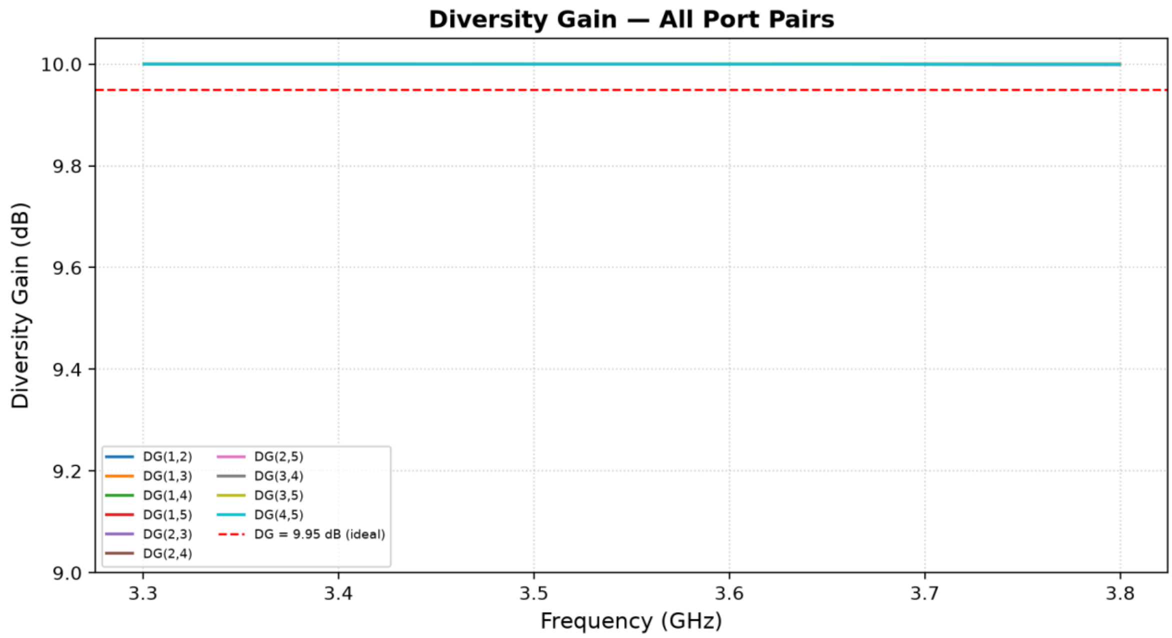

Fig. 15: Diversity Gain (DG)

The third parameter is channel capacity Loss (CCL). The CCL measures the degradation in channel capacity due to antenna correlation. Fig 16 shows CCL remains below 0.4 bps/Hz/s for all port pairs across the 3.42-3.51Ghz band, well within the acceptable limit of 0.4 bps/Hz/s. This CCL confirms that the proposed multi-sector configuration is significantly suitable for the channel capacity of a 5G MIMO system.

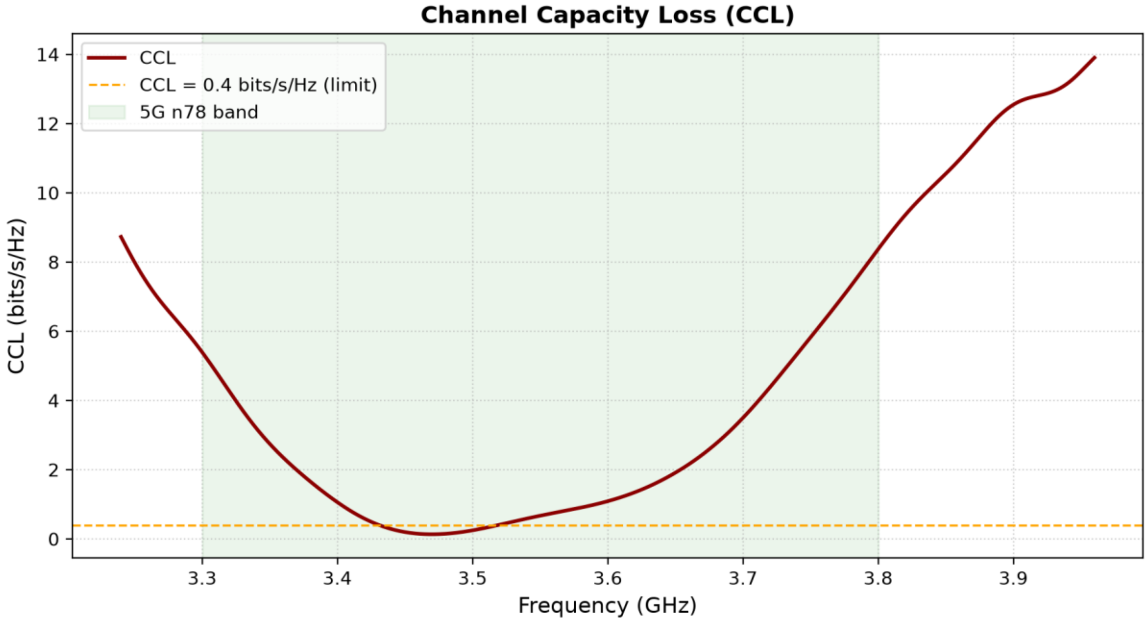

Fig. 15: Channel Capacity Loss (CCL)

The fourth parameter is total active reflection Coefficient (TARC), which is accounts for the combined effect of all S-parameters and is a more comprehensive measure of multi-port matching than individual Sii values. Fig. 16 shows TARC < −10 dB for all five ports, confirming excellent active impedance matching in the multi-port configuration.

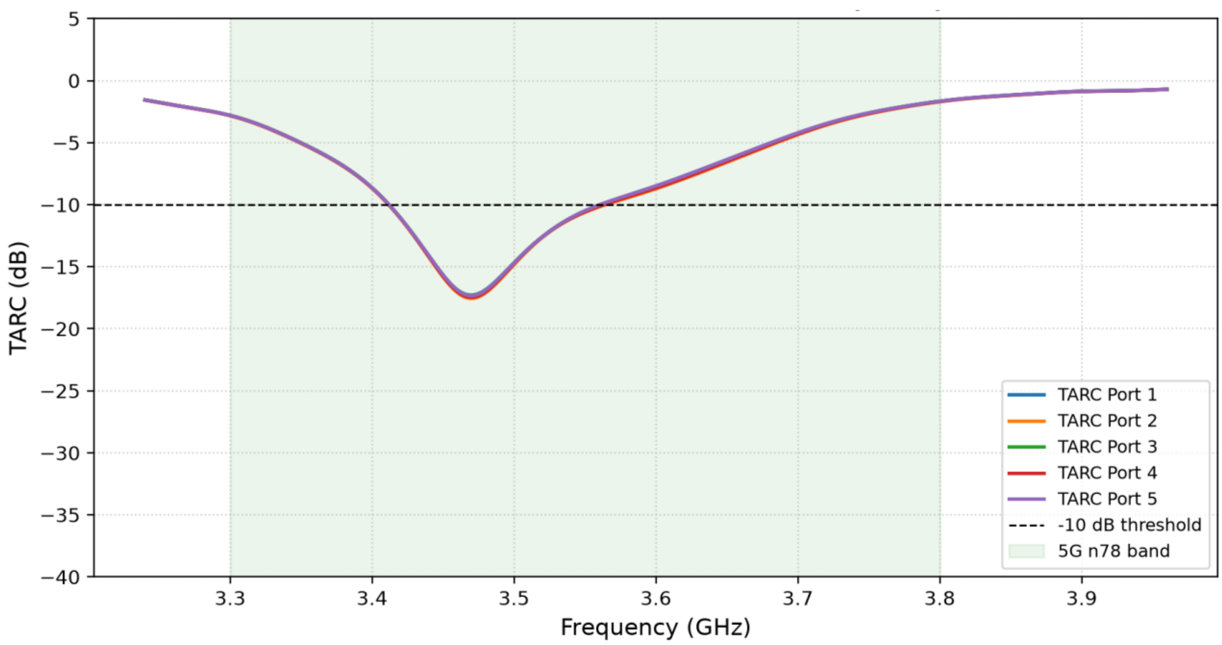

Fig. 16: Total Active Reflection Coefficient (TARC)

5. Conclusion

All results presented in this paper are obtained from full-wave electromagnetic simulation using CST Microwave Studio. Fabrication and measurement validation are planned as future work to validate the simulation results.
The desired antenna, which is presented in this study by using the CST studio program, showed an excellent performance characteristic suitable for a 5G base station antenna, especially in a good gain with an 360° radiation pattern. Using five. All results were simulated at a frequency of 3.5 GHz, which is in (n78) band that is used in 5G.
Table 1 shows a comparison between the desired antenna and three articles at the same frequency. The main specification for our antenna is the circular polarization and radiation pattern because it covers 360° and suitable for 5G stations.
The antenna showed excellent impedance matching (S11) and a bandwidth of 160 MHz Every sector in antenna array provides a gain of 9 dB is higher than single-patch designs, illustrating the effectiveness of every sector in the array design in achieving directional radiation.
Using five sectors in antenna design enables 360-degree coverage, making it suitable for macro cell deployment. The radiation pattern for every sector with a 72-degree HPBW in the azimuth plane provides a coverage overlap between adjacent sectors while minimizing interference.

Table 1: The comparison between the desired antenna and other antennas

Parameter	This work	Al-Bawri SS et al[24]	Ghaoual FE et al[14]	Alwareth H et al[25]
Antenna structure	5sectors× 4	8 subarrays × 2	64elements	1 × 4 array
Antenna size(mm^2)	~266×53	~300×200	~200×100	~150×80
Antenna type	Microstrip patch array	mMIMO with MTM	Active planar patch	microstrip array antenna
BW(MHz)	160	300	500	60
Gain	9dBi	19.5 dBi	17.5 dBi	11.4 dBi @ 3.5 GHz
Eff (%)	>90	~88	~90	~77
Polar	Circular	Linear	Linear	Linear
Isolation(dB)	>20	>20	N/A	N/A
Radiation coverage	360°	directive	directive	directive

References

[1] 3GPP(2022), NR and NG-RAN Overall Description.

[2] A. Gupta, and R. K. Jha (2015), A survey of 5G network, Architecture and emerging technologies. *IEEE access*, vol. 3, pp. 1206-1232. https://doi.org/10.1109/access.2015.2461602.

[3] I. Zewail, S. Mohsen, and M. M. Zayed(2026), Design and Implementation of a Compact 20-Port Wideband MIMO Antenna Array for 5G/6G Indoor Base Stations. *Wireless Personal Communications*, pp. 1-32. https://doi.org/10.1007/s11277-025-11901-5.

[4] 3gpp (2023), NR; User Equipment (UE) radio transmission and reception.

[5] 5G Spectrum Guide. https://www.gsma.com/connectivity-for-good/spectrum/5g-spectrum-guide-2/.

[6] C. A. Balanis (2016), Antenna theory: analysis and design .*John wiley & sons*.

[7] T. S. Rappaport, S. Sun, R. Mayzus, H. Zhao, Y. Azar, K. Wang, G. N. Wong, J. K. Schulz, M. Samimi, and F. Gutierrez (2013), Millimeter wave mobile communications for 5G cellular: It will work. *IEEE access*, vol. 1, pp. 335-349. https://doi.org/10.1109/access.2013.2260813.

[8] A. A.-K. Salih, M. Nangir, and A. Pourziad (2026), MM Wave (4× 1) MIMO Planar Printed Antenna with High Isolation Using a Hashtag-Like Decoupling Technique for 5G Applications. *Journal of Electrical Engineering & Technology*, pp. 1-17. https://doi.org/10.1007/s42835-025-02578-8.

[9] S. A. Alassawi, W. A. Ali, N. Ismail, and M. R. Rizk (2023), Compact elliptic ring 2× 2 and 4× 4 MIMO-UWB antenna at 60 GHz for 5G mobile communications applications. *Microsystem Technologies*, vol. 29, no. 4, pp. 431-440. https://doi.org/10.1007/s00542-022-05383-9.

[10] R. Schulpen, U. Johannsen, S. Pires, and A. Smolders (2018), Design of a phased-array antenna for 5G base station applications in the 3.4-3.8 GHz band. p. 743. https://doi.org/10.1049/cp.2018.1102.

[11] L. Li, D. Wang, X. Niu, Y. Chai, L. Chen, L. He, X. Wu, F. Zheng, T. Cui, and X. You (2018), mmWave communications for 5G: implementation challenges and advances. *Science China Information Sciences*, vol. 61, no. 2, pp. 021301. https://doi.org/10.1007/s11432-017-9262-8.

[12] P. Mounika, and T. Jaya (2025), Design of 4X4 Microstrip patch array antenna for 5G MMWave applications. *SSRG International Journal of Electronics and Communication Engineering*, vol. 12, no. 1, pp. 104-117. https://doi.org/10.14445/23488549/ijece-v12i1p108.

[13] M. S. Rana, and M. M. R. Smieee (2022), Design and analysis of microstrip patch antenna for 5G wireless communication systems, *Bulletin of Electrical Engineering and Informatics*, vol. 11, no. 6, pp. 3329-3337. https://doi.org/10.11591/eei.v11i6.3955.

[14] F. El Ghaoual, J. Zbitou, M. Hefnawi, and A. El Hammoumi (2025), A compact active planar patch antenna array for sub-6 ghz 5g applications. *e-Prime-Advances in Electrical Engineering, Electronics and Energy*, vol. 11, pp. 100903. https://doi.org/10.1016/j.prime.2025.100903.

[15] R. N. Tiwari, D. Sharma, P. Singh, and P. Kumar (2024), A flexible dual-band 4× 4 MIMO antenna for 5G mm-wave 28/38 GHz wearable applications. *Scientific reports*, vol. 14, no. 1, pp. 14324. https://doi.org/10.1038/s41598-024-65023-2.

[16] S. I. Siddiqui, S. Bashir, A. Khan, S. Ghafoor, and I. Aziz (2024), A dual-band high-gain beam steering antenna array for 5G sub-6 GHz base station. *Scientific Reports*, vol. 14, no. 1, pp. 26517. https://doi.org/10.1038/s41598-024-75822-2.

[17] Y. N. University. Small, Efficient 5G Multisector Antenna Indoor Base Station Achieves World's First Demonstration using 28GHz.

[18] S. K. Noor, N. Ramli, N. M. Sahar, and T. Khalifa (2008), Compact and wide bandwidth microstrip patch antenna for 5G millimeter wave technology: Design and analysis. p. 012008. https://doi.org/10.1088/1742 6596/1878/1/012008.

[19] Microstrip Patch Antenna, https://www.geeksforgeeks.org/electronics-engineering/microstrip-patch-antenna/.

[20] R. Garg (2001), Microstrip antenna design handbook. *Artech house*.

[21] D. M. Pozar (2011), Microwave engineering. *John wiley & sons*.

[22] W. L. Stutzman, and G. A. Thiele (2012), Antenna theory and design. *John Wiley & Sons*.

[23] C. A. Balanis (2012), Advanced engineering electromagnetics. *John Wiley & Sons*.

[24] S. S. Al-Bawri, M. T. Islam, M. S. Islam, M. J. Singh, and H. Alsaif (2022), Massive metamaterial system-loaded MIMO antenna array for 5G base stations, *Scientific Reports*, vol. 12, no. 1, pp. 14311. https://doi.org/10.1038/s41598-022-18329-y.

[25] H. Alwareth, I. M. Ibrahim, Z. Zakaria, A. J. A. Al-Gburi, S. Ahmed, and Z. A. Nasser (2022), A wideband high-gain microstrip array antenna integrated with frequency-selective surface for Sub-6 GHz 5G applications. *Micromachines*, vol. 13, no. 8, pp. 1215. https://doi.org/10.3390/mi13081215.